ELSEVIER

Biochimica et Biophysica Acta 1414 (1998) 108–126

BIOCHIMICA ET BIOPHYSICA ACTA
BBA

The interaction of *Staphylococcus aureus* bi-component γ-hemolysins and leucocidins with cells and lipid membranes

Mercedes Ferreras [a], Frank Höper [a], Mauro Dalla Serra [a], Didier A. Colin [b], Gilles Prévost [b], Gianfranco Menestrina [a,*]

[a] *CNR-ITC Centro Fisica Stati Aggregati, Via Sommarive 18, I-38050 Povo (Trento), Italy*
[b] *LTAB (UPRES-EA 1318) Institut de Bactériologie de la Faculté de Médecine, Université Louis Pasteur, Rue Koeberlé 3, F-67000 Strasbourg, France*

Received 11 June 1998; received in revised form 7 August 1998; accepted 24 August 1998

Abstract

Staphylococcus aureus γ-hemolysins (HlgA, HlgB and HlgC) and Panton-Valentine leucocidins (LukS-PV and LukF-PV) are bi-component toxins forming a protein family with some relationship to α-toxin. Active toxins are couples formed by taking one protein from each of the two subfamilies of the S-components (LukS-PV, HlgA and HlgC) and the F-components (LukF-PV and HlgB). We compared the mode of action of the six possible couples on leukocytes, red blood cells and model lipid membranes. All couples were leucotoxic on human monocytes, whereas only four couples (HlgA+HlgB, HlgC+HlgB, LukS-PV+HlgB and HlgA+LukF-PV) were hemolytic. Toxins HlgA+HlgB and HlgC+HlgB were also able to induce permeabilisation of model membranes by forming pores via oligomerisation. The presence of membrane-bound aggregates, the smallest and most abundant of which had molecular weight and properties similar to that formed by α-toxin, was detected by SDS-PAGE. By infrared spectroscopy in the attenuated total reflection configuration (FTIR-ATR), the secondary structure of both components and of the aggregate were determined to be predominantly β-sheet and turn with small variations among different toxins. Polarisation experiments indicated that the structure of the membrane complex was compatible with the formation of a β-barrel oriented perpendicularly to the plane of the membrane, similar to that of porins. The couple LukS-PV+LukF-PV was leucotoxic, but not hemolytic. When challenged against model membranes it was able to bind to the lipid vesicles and to form the aggregate with the β-barrel structure, but not to increase calcein permeability. Thus, the pore-forming effect correlated with the hemolytic, but not with the complete leucotoxic activity of these toxins, suggesting that other mechanisms, like the interaction with endogenous cell proteins, might also play a role in their pathogenic action.

Keywords: Staphylococcal leucotoxin; Hemolysis; Toxin pore; Phospholipid bilayer; Fourier-transform infrared spectroscopy; Unilamellar vesicle; Calcein release; Bi-component action; (*Staphylococcus aureus*)

Abbreviations: PC, phosphatidylcholine; Cho, cholesterol; TLC, thin layer chromatography; SUV, small unilamellar vesicles; RRBC, rabbit red blood cells; HRBC, human red blood cells; PVL, Panton-Valentine leucocidin; PBS, phosphate buffered saline; FCS, fetal calf serum; SDS, sodium dodecyl sulfate; Triton X-100, octylphenoxy polyethoxy ethanol; Lubrol-PX, polyethyleneglycol(9)dodecyl ether; DOC, deoxycholate; PAGE, polyacrylamide gel electrophoresis; FTIR, Fourier-transform infrared spectroscopy; ATR, attenuated total reflection

* Corresponding author. Fax: +39 (461) 810628; E-mail: menes@cefsa.itc.it

0005-2736/98/$ – see front matter
PII: S0005-2736(98)00160-6

1. Introduction

Staphylococcus aureus produces several toxic pore-forming compounds involved in a number of pathologies of humans and cattle, of which α-toxin and δ-lysin are perhaps the best characterised [1]. Among these toxins, leucocidins and γ-hemolysins share the peculiarity of being bi-component. They are constituted by two proteins that after being synthesised and secreted separately, as totally inactive components, act synergically to efficiently damage some mammalian cells. Since the discovery of leucocidins by Panton et al. in 1932 [2], the number of bi-component toxins belonging to this group has grown constantly and at least 11 members are known to date [3]. With the availability of their primary sequence, it became evident that staphylococcal leucocidins and γ-hemolysins were actually forming a single family and were also related to α-toxin [4,5]. LukS-PV, HlgA and HlgC present around 63–75% of sequence identity among them, and slightly lower when compared with LukF-PV or HlgB. On the other hand, LukF-PV and HlgB are around 70% identical. Consequently, this family of proteins is divided into two sub-families: the class S components, which include LukS-PV, HlgA and HlgC, and the class F components, including LukF-PV and HlgB. Synergically active couples always include one S component plus one F component. Interestingly, α-toxin has around 26–30% of sequence identity with class F components and 20–25% with class S components.

The mode of action of the Panton-Valentine leucocidin (PVL) has been reasonably well established. It was demonstrated that binding of the two components to the cell has a sequential character, so that the initial binding of the S component allows the subsequent binding of the F component on rabbit red blood cells (RRBC) and human polymorphonucleated cells [6,7]. However, for the couple HlgA+HlgB acting on human red blood cells (HRBC), a reverse binding sequence was reported [8,9]. The leucotoxic activity of PVL seems to be mediated by the opening of pores in the target membrane, whose formation involves toxin oligomerisation [10,11]. A hexamer has been recently described [12], although a trimer was also reported earlier [8].

The permeability of the pore depends on the concentration of divalent cations in the extracellular medium [7]. With concentrations of calcium lower than 1 mM, the induced lesions are big enough to allow the leakage of intracellular components which eventually causes cell death by osmotic shock. In the presence of concentrations of calcium higher than 1 mM, the lesions induced by PVL are essentially ion-sized pores, permeable to different divalent cations. An influx of calcium induces intracellular events, such as degranulation, secretion, activation of phospholipase A_2, release of leukotriene B_4 with subsequent inflammation processes and chemotaxis of neutrophils and eosinophils, as well as DNA fragmentation [7,11,13,14].

Since the V8 strain (ATCC 49775) produces both PVL and γ-hemolysins [15], the possibility to find leucotoxic or hemolytic activity in mixed couples containing one leucocidin protein plus one γ-hemolysin protein was open. Indeed, it was found that the mixed couple HlgA+LukF-PV presented both toxic activities, whereas the couples HlgC+LukF-PV and LukS-PV+HlgB presented only leucotoxic properties [15]. It was inferred that the S component is responsible for the selectivity of the couple, concluding that HlgA and HlgC are able to bind to both red and white cells, whereas LukS-PV derived couples can attack only white cells.

Despite the relative abundance of data on the activity of these toxins on sensitive cells, up to now no study was reported on their action on model membranes. Here we present an investigation, performed with all the six possible couples formed by one S plus one F component, which compares the permeabilisation of model membranes (lipid vesicles) with the leucotoxic and hemolytic activity and allows to better understand their mechanism of action. The use of this simple model system demonstrated the presence of a hexameric form inserted into the membrane, which appears to constitute the species out of which the pore is formed. The stoichiometry of the two components of the couple in the oligomer was determined as well as the secondary structure of every single component and of the membrane bound oligomer.

2. Materials and methods

2.1. Chemicals

Lipids used were phosphatidylcholine (PC), purchased by Avanti Polar Lipids, and cholesterol (Cho) by Fluka, both more than 99% pure by TLC. Calcein, EDTA, Sephadex, Dulbecco's medium (PBS) and RPMI 1640 medium were from Sigma, SDS and Lubrol from Pierce, Triton X-100 from Merck, and alamar Blue from Alamar Bio-Sciences. The preparation and purification of single leucotoxin components has been described earlier [15,16]. Lyophilised α-toxin was kindly supplied by Dr. Hungerer (Behring, Marburg, Germany), and used without further purification.

2.2. Determination of the hemolytic activity

Rabbit red blood cells (RRBC) were prepared from fresh venous blood collected in 6 mM EDTA, and washed thrice (10 min centrifugation at $700\times g$, room temperature) in 30 mM Tris-HCl, 100 mM NaCl, 1 mM EDTA, pH 7.0 (hereafter buffer A). Human red blood cells (HRBC) from healthy volunteers, were prepared similarly.

2.2.1. Kinetic experiments

The time course of hemolysis was followed photometrically at 650 nm, in a 96-well microplate, as described earlier [17]. In each well, the couple of proteins was added (both components at the same molar concentration if not otherwise stated) in a final volume of 100 μl of buffer A. Toxins were two-fold serially diluted and the reaction was started by adding 100 μl of RRBC (or HRBC), at a final concentration of 0.13% (v/v), which corresponds to an initial A_{650} value of 0.1. The microplate was stirred and read every 8 s for 45 min. The extent of hemolysis was calculated as follows:

$$\%\ \text{hemolysis} = 100(A_i - A_f)/(A_i - A_w) \quad (1)$$

where A_i and A_f are the absorbances at the beginning and at the end of the reaction, and A_w that obtained after hypotonical lysis with pure water. The maximal rate of hemolysis (V_{max}) was calculated, as the largest slope in the absorbance vs. time curve.

2.2.2. Endpoint experiments

Toxins were incubated with 0.13% RRBC (v/v), in 500 μl of buffer A for 15 min at 37°C (unless specified differently). Thereafter, intact cells were pelleted ($15\,800\times g$, 3 min), and the released hemoglobin was measured by the absorbance at 415 nm. The extent of hemolysis was calculated as follows:

$$\%\ \text{hemolysis} = 100(A_+ - A_-)/(A_w - A_-) \quad (2)$$

where A_+ and A_- are the absorbances of the sample with and without toxin, and A_w is defined as above. Binding sequence assays were performed as two consecutive end-point measurements, by adding to the same cells one single component at each step. An end-point assay was also used to study the temperature dependence of the permeabilising activity. Samples containing both leucotoxin components were in this case incubated at different temperatures, and thereafter treated at 0°C.

2.3. Determination of the leucotoxic activity

In vitro cytotoxic activity was studied on different human leukocytes: freshly isolated human monocytes, THP-1 cells (ATCC TIB 202, leukemic monocytes from a human newborn) and Raji cells (ATCC CCL 86, lymphocytes from human Burkitt lymphoma) both obtained from the American Type Culture Collection (Bethesda, MA, USA). To monitor cell growth we used a photometric assay based on the alamar Blue reagent [18]. The reduction of this dye by living cells can be detected by measuring the difference in absorbance at 575 nm and 608 nm ($A_{575}-A_{608}$). The assay was performed in a 96-well microplate. Along each line, toxins were two-fold diluted and incubated with 1×10^5 cells and 2.5% (v/v) alamar Blue, in RPMI-1640 medium without phenol red. The final volume in each well was 200 μl. The microplate was maintained at 37°C, under a humidified 5% CO_2 atmosphere, and read every 30 min, for a total of 30 h, in a microplate reader (UVmax from Molecular Devices).

2.3.1. Preparation of monocytes from blood

Blood was collected in heparin (1000 U/ml), diluted in Dulbecco's phosphate buffered saline medium, and fractionated by centrifugation ($400\times g$, for 30 min), on 33% Ficoll (v/v). The band of mono-

cytes plus lymphocytes was carefully collected and washed twice in RPMI-1640 ($280\times g$, 10 min). Cells were placed in a 96-well microplate, 1.2×10^5 cells per well, and allowed to adhere for 1 h. Non-adherent lymphocytes were carefully washed out while monocytes, attached to the bottom of the wells, were incubated overnight in a medium containing 8.76% RPM1 1640 (v/v) supplemented with 2% glutamine, 0.4% gentamicin and 10% FCS (37°C, 5% CO_2), and used for the cytotoxicity assay. Other cell lines were maintained in the same supplemented RPMI-1640 medium (37°C, 5% CO_2) until assayed.

2.4. Permeabilisation of lipid vesicles

Small unilamellar vesicles (SUV) comprised of PC/Cho at different ratios were prepared by sonication of multilamellar liposomes (2 mg of total lipid/ml of suspension) for 1 h, in a solution containing 80 mM calcein (from Sigma), neutralised with NaOH. Titanium particles released by the sonotrode were eliminated by centrifugation. The untrapped dye was removed by washing on Sephadex G-50, with buffer A. The permeabilising activity of toxins on SUV was evaluated by measuring the release of calcein [19]. Aliquots of washed SUV were placed in a 1-cm stirred plastic cuvette, in a total volume of 1.2 ml of buffer A. The final lipid concentration was 20 μg/ml, unless otherwise stated. After adding the two components of the couple, always at the same concentration, the time-course of calcein release was recorded by the increase in the fluorescence emitted at 520 nm (excitation at 494 nm), because of the dequenching of the released dye which dilutes in the external medium. Toxin induced permeabilisation was calculated as:

$$P(\%) = 100(F_t - F_i)/(F_m - F_i) \quad (3)$$

where F_i is the initial fluorescence before adding the toxins, F_t the value at time t, and F_m the maximal value after addition of 1 mM Triton X-100. Spontaneous release of calcein was negligible.

2.5. Theoretical model for the interpretation of SUV permeabilisation

The release data were analysed in terms of a statistical model that we have thoroughly described recently [20]. It was derived from that originally presented by Parente et al. [21] and later improved by Rapaport et al. [22]. For the sake of clarity, we summarise here the main assumptions and the basic equations on which it relies.

The process of permeabilisation is divided in two steps: partitioning of toxin monomers into the lipid bilayer (assumed to be very fast), and aggregation of membrane-inserted monomers (assumed to be rate limiting). When an aggregate has reached a critical size, comprising M monomers, a conducting unit is formed and internal calcein is quickly released. The fate of the oligomer after this step does not influence the release process any more, since the vesicle is already empty. For example it can enter an irreversible state, as in the case of α-toxin, and this would not affect the treatment. The equilibrium constant of the incorporation process is given by:

$$K_1 = \frac{T_b}{(T_0 - T_b)\cdot L} \quad (4)$$

where T_0 and L are the total concentration of toxin and lipid respectively and T_b is the concentration of bound toxin. The aggregation process is instead characterised by c, the forward rate constant, and d, the backward rate constant. For simplicity they are assumed to be independent of the component that adds to the oligomer and of the degree of aggregation. The equilibrium constant is in this case:

$$K_2 = \frac{c}{d}. \quad (5)$$

The percentage of calcein release is given by:

$$P(\%) = 100\sum_{i=M}^{N} A_i \cdot Z(M, t, i, K_2, c) \quad (6)$$

where A_i is the fraction of vesicles with i monomers bound, N is the maximum number of toxin molecules that can be bound to one vesicle, and $Z(M,t,i,K_2,c)$ is the probability that a vesicle containing i bound monomers will also have an aggregate of order not smaller than M at time t.

Resulting from the fast partitioning step, A_i is time independent. Its expression can be derived from a binomial distribution [20,21]. All of the time dependence is contained in the probability factor Z, that can be expressed as [22]:

$$Z(M,t,i,K_2,c) = p(t)^{M-1}(M-(M+1)\cdot p(t)) \quad (7)$$

where

$$p(t) = \frac{1}{K + \sqrt{K^2-1}\coth\left(c\cdot i\cdot t\sqrt{K^2-1}\right)} \quad (8)$$

and

$$K = 1 + \frac{1}{4iK_2}. \quad (9)$$

2.6. Preparation of toxin oligomers on SUV

PC/Cho SUV (1:1 molar ratio) were prepared by sonication of a 6 mg/ml suspension of the lipids in a buffer containing 10 mM HEPES at pH 7.0 (buffer B). Aliquots of these vesicles were diluted to a 3 mM lipid concentration, and incubated with 7.5 μM of each component of the toxin couple in 200 μl of buffer B (final molar ratio lipid/toxin 200:1). After incubation at 37°C for 1 h, free toxins were washed out by ultrafiltration through polysulfone filters of 300 kDa cut-off (NMWL, Millipore) using 2000×*g* for 20 min. The filtrates were tested for the presence of free toxins by measuring the hemolytic activity on RRBC. The washing process was repeated several times, adding 200 μl of buffer B each time, until there was no more hemolytic activity eluting in the filtrates. The presence of toxins in the filtrates was also tested at each step by SDS-PAGE. The retentates, consisting of permeabilised vesicles and bound toxin, were then collected in the same buffer, and subjected to SDS-PAGE and FTIR analysis.

2.7. SDS-electrophoresis

Electrophoresis was performed under denaturing conditions [23] using precast polyacrylamide minigels (Pharmacia, Uppsala, Sweden), with density gradients ranging from 4 to 15% or from 10 to 15%. Protein samples were dissolved in a buffer containing 2.5% SDS (w/v) and boiled for 5 min, unless otherwise specified. In the case of samples containing toxins incubated with lipid vesicles, the preparations were also supplemented with 0.1 mg/ml Lubrol (Pierce) to better solubilise the toxins from the membrane. Electrophoresis was run at 10°C in a buffer containing 0.5% SDS (w/v), in a semi-automatic horizontal apparatus (Phastsystem by Pharmacia). Gels were stained with Coomassie brilliant blue or silver stain. The amount of protein was quantitated in Coomassie-stained gels by bidimensional densitometry, using a PhastImage densitometer (Pharmacia), with a band-pass filter at 613 nm.

2.8. Fourier-transform infrared spectroscopy

FTIR spectra were collected in the attenuated total reflection (ATR) configuration [24–26] on a Bio-Rad FTS 185 spectrometer equipped with a DTGS detector with CsI window, a KBr beamsplitter and an ATR attachment by Specac. The instrument was constantly purged with dry air. Depending on the intensity of the signal, 64–256 interferograms were collected, Fourier transformed and averaged. Absorption spectra in the region between 4000 and 1000 cm^{-1}, at a resolution of one data point every 0.25 cm^{-1}, were obtained using a clean ATR crystal as the background. For the study of single leucotoxin components, or their bi-component combination, 40 μl of a solution containing approximately 1 mg/ml of protein extensively dialysed against three changes of buffer B, were deposited and dried in a thin layer on one side of a 10-reflections Ge crystal (45° cut). For the lipid-bound toxin, 40 μl of the toxin-treated and extensively washed SUV preparation described above, were spread similarly. For control experiments toxin-free SUV were also applied in the same way. The crystal was housed in a liquid cell and flushed with D_2O-saturated nitrogen for 45 min before collecting the reported spectra. Spectra were also collected during the deuteration process to verify that a steady state was attained [27].

The ATR-FTIR spectra were processed using Bio-Rad Win-Ir software package. They were corrected by subtracting the absorbance of residual H_2O (to give a smooth baseline between 2000 and 1700 cm^{-1}), and a linear baseline between 1720 and 1500 cm^{-1}. At this point, the amide I′ band, between 1700 and 1600 cm^{-1}, was curve-fitted with a sum of Lorentzians using the Levenberg-Marquardt method, with no constrained parameter. The starting parameters, i.e. the initial number, position, amplitude and width of the Lorentzians, was derived from the anal-

ysis of the deconvoluted spectrum [24,26]. The relative content of secondary structure elements was eventually estimated by the areas of the individual peaks, assigned to a particular secondary structure in the standard way [24,28], and normalised by dividing by the area of the whole amide I′ band. The small components around 1610 cm^{-1}, resulting from the contribution of side chains [29], were excluded from the analysis. In the case of lipid-bound toxin, spectra were first corrected by subtracting the contribution of the lipid alone (minimising the signal of the phospholipid carboxyl groups at 1738 cm^{-1}), and then analysed as above, or, alternatively, used to produce a differential spectrum by subtracting the spectrum of the pure bi-component couple, weighted by the area of the amide I′ band.

2.9. Quantitative analysis of the polarised ATR-IR spectra

In the case of the lipid-bound leucotoxin couples the orientation of the various structural elements was determined by polarisation experiments. A rotating wire-grid polariser from Specac was used and manually positioned with orientation either parallel (∥) or perpendicular (⊥) to the plane of the internal reflections. The dichroic ratio was calculated as $R = A_{\parallel}/A_{\perp}$, where $A_{\parallel}$ and $A_{\perp}$ were the integrated absorption bands in the parallel and perpendicular configuration, respectively. From the dichroic ratio a form factor, S, was calculated as [25,30,31]:

$$S = \frac{E_x^2 - RE_y^2 + E_z^2}{1/2(3\cos^2\alpha - 1)(E_x^2 - RE_y^2 - 2E_z^2)} \quad (10)$$

where α is the angle between the long axis of the molecule under consideration and the transition moment pertaining to the investigated vibration; E_x, E_y and E_z are the components of the electric field of the evanescent wave along the three directions (the z axis is chosen perpendicular to the plane of the crystal). The terms E_x^2, E_y^2 and E_z^2 were calculated according to the expressions given by Harrick [30,31] for thick films [32] using the following values: refractive index of the Ge crystal 4, refractive index of the deposited layer 1.43, incidence angle 45°. The expression above was used to calculate the order parameters for: (i) the lipid chains (S_L), using the symmetric and asymmetric CH_2 stretching, i.e. integrating the bands centred at 2850 and 1918 cm^{-1}, respectively, with $\alpha = 90°$; (ii) the whole amide I′ band ($S_{amideI'}$), integrating between 1600 and 1700 cm^{-1}, with $\alpha = 0°$ [33,34]; (iii) the β strands (S_β), summing the Lorentzian components pertaining to β^1 and β^2 structures and using $\alpha = 70°$ [34].

From the order parameter the average tilt angle γ of the molecular axis with respect to the z axis (i.e. the perpendicular to the plane of the membrane) can be calculated according to [31]:

$$S = \frac{1}{2}(3\cos\gamma - 1). \quad (11)$$

$A_{\perp}$ was also used to calculate the lipid to toxin ratio (L/T) using the following algorithm, according to [33,34]:

$$L/T = 0.208\frac{(n_{res}-2)}{2}\frac{1-S_{amideI'}}{1+S_L/2}\frac{\int_{2800}^{2980} A_{\perp}(\nu_L)d\nu}{\int_{1600}^{1690} A_{\perp}(\nu_{amideI'})d\nu} \quad (12)$$

where n_{res} is the total number of residues in the couple, S_L and $S_{amideI'}$ have been defined above.

Fig. 1. Titration of the four bi-component toxins having hemolytic activity on red blood cells. A: Extent of hemolysis of rabbit RBC, expressed as a percentage of that obtained by incubating with distilled water. Different symbols have been used for different couples, as indicated. Points are mean ± S.D. of 3 independent experiments. Curves were best fit of the Hill equation providing the following coefficients: HlgA+HlgB, 3.2; HlgC+HlgB, 1.7; LukS-PV+HlgB, 1.5; HlgA+LukF-PV, 1.8. Inset: Similar experiments, but with human RBC (the same symbols have been used). Only the couple HlgA+HlgB was active, with a Hill coefficient 2.9. All other couples were inactive, albeit only HlgC+HlgB is shown. B: Maximal rate of hemolysis (V_{max}) calculated from the kinetic curves of hemolysis. Symbols and inset have the same meaning as in part A. Lines have no theoretical significance here. The S and F component were always applied at the same, reported, concentration. The time course of hemolysis was followed turbidimetrically at 650 nm, and the final % of hemolysis and V_{max} were calculated as described in Section 2.

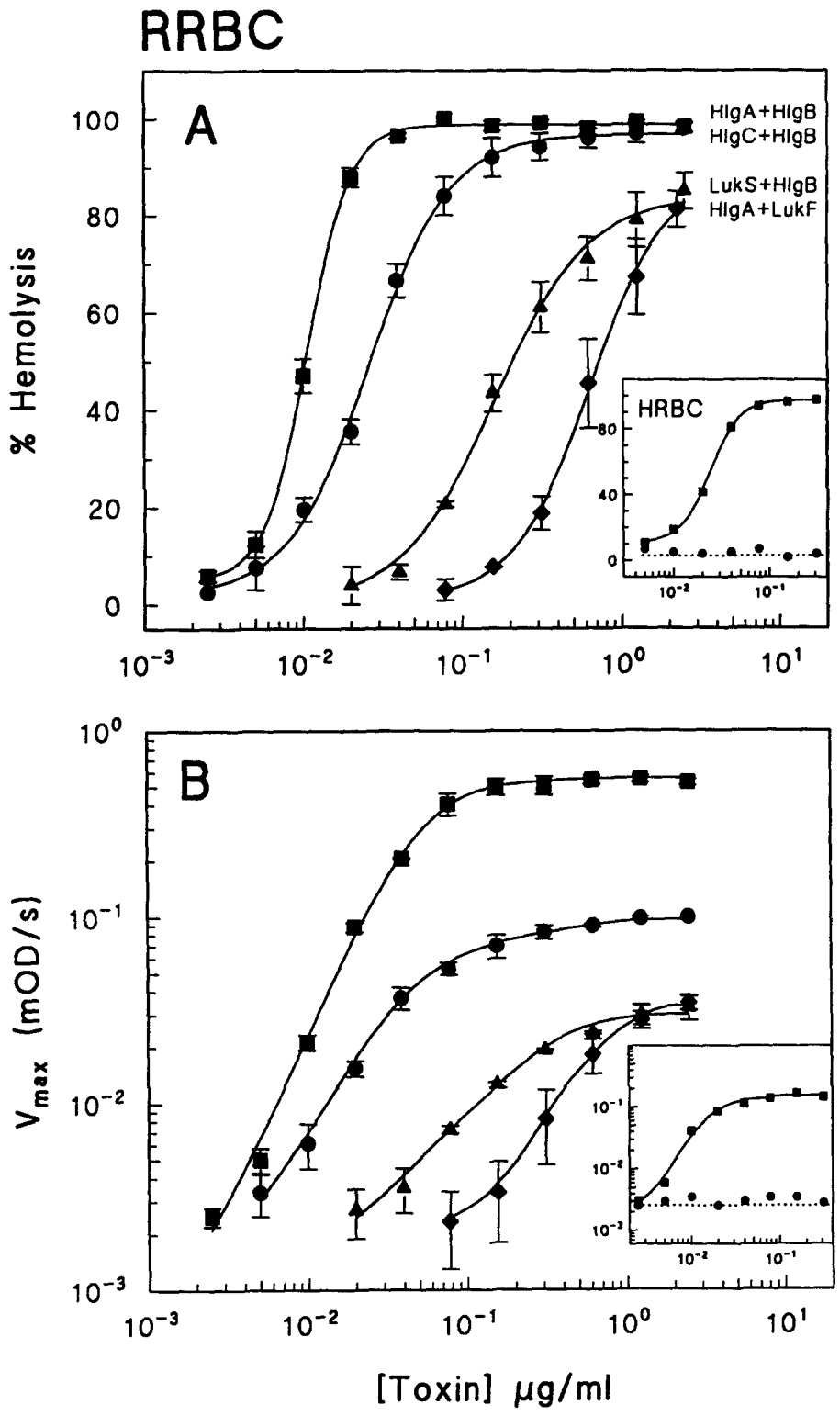
RRBC
A
HlgA+HlgB
HlgC+HlgB
LukS+HlgB
HlgA+LukF
HRBC
% Hemolysis
B
V_{max} (mOD/s)
[Toxin] µg/ml

3. Results

3.1. Hemolytic activity

The hemolytic activity of the six bi-component leucotoxins formed by taking one S component plus one F component from the γ-lysin and the PVL of strain ATCC 49775, was assayed on rabbit and human RBC, in terms of percentage and maximal rate (V_{max}) of hemolysis (Fig. 1). Four couples (HlgA+HlgB, HlgC+HlgB, LukS-PV+HlgB and HlgA+LukF-PV) presented hemolytic activity against rabbit RBC, whereas only HlgA+HlgB was active on human erythrocytes (insets). The hemolytic activity of the couple LukS-PV+HlgB was never reported before. The relative hemolytic efficiency of these toxins are reported in Table 1, by comparing the concentration of protein needed to give 50% of the maximal hemolysis ($C_{50\%}$), and the upper limit of V_{max} (V_{lim}). On RRBC, HlgA+HlgB had the strongest hemolytic activity, followed by HlgC+HlgB, LukS-PV+HlgB and finally HlgA+LukF-PV. As indicated by V_{lim} values, HlgA+HlgB also expresses the fastest kinetics, followed by the others in the same order as above. On HRBC, the hemolytic activity of HlgA+HlgB was only about 50% of that on RRBC. For comparison, the hemolytic activity of α-toxin is also reported, under the same experimental conditions.

The sequentiality of binding to both rabbit and human RBC was studied for all the active couples (i.e. HlgA+HlgB, HlgC+HlgB, LukS-PV+HlgB and HlgA+LukF-PV on RRBC, and HlgA+HlgB on HRBC). Erythrocytes were incubated consecutively with the two components in both possible orders. After addition of the first component, cells were washed thrice, to remove the unbound protein. In all cases, (including HlgA+HlgB on HRBC), release after the first addition was nil and hemolysis finally ensued only if (and every time) the S component was applied first. The temperature dependence of the hemolytic activity on RRBC was next analysed. For HlgA+HlgB, HlgC+HlgB, and LukS-PV+HlgB, the activity increased progressively from 0°C to 37°C, whereas in the case of HlgA+LukF-PV, the activity at 20°C was higher than either at 37°C or at 0°C. No significant hemolysis was observed when any of the four toxin couples was added at 0°C. However, hemolysis ensued immediately if the cells, washed at 0°C, were brought to 37°C. This suggests that the two components can indeed bind irreversibly to the cell during the incubation at 0°C, although the progress to the active lesion is only possible at normal temperature.

Table 1
Hemolytic and leucotoxic activity of the bi-component toxins and α-toxin

		S component F component	HlgA HlgB	HlgC HlgB	LukS-PV HlgB	HlgA LukF-PV	HlgC LukF-PV	LukS-PV LukF-PV	α-Toxin
Hemolytic activity	RRBC	$C_{50\%}$ (ng/ml)	10 ± 1	26 ± 1	160 ± 20	630 ± 50	0	0	62 ± 2
		V_{lim} (μOD/s)	540 ± 6	102 ± 3	36 ± 2	38 ± 3	0	0	229 ± 14
	HRBC	$C_{50\%}$ (ng/ml)	25 ± 3	0	0	0	0	0	0
		V_{lim} (μOD/s)	150 ± 5	0	0	0	0	0	0
Leucotoxic activity	Monocytes	$C_{50\%}$ (ng/ml)	217 ± 27	14 ± 2	14 ± 3	177 ± 20	14 ± 5	3 ± 1	44 ± 1
		% Cell death$_{max}$	84.8 ± 3.5	54.3 ± 1.6	54.0 ± 2.2	64.1 ± 2.4	49.3 ± 3.5	52.9 ± 0.0	87.6 ± 1.0
	THP1	$C_{50\%}$ (ng/ml)	39 ± 2	0	0	155 ± 10	0	0	480 ± 21
		% Cell death$_{max}$	73.1 ± 3.5	0	0	92.3 ± 2.4	0	0	69.2 ± 1.6
	RAJI	$C_{50\%}$ (ng/ml)	150 ± 25	0	0	820 ± 55	0	0	9750 ± 325
		% Cell death$_{max}$	63.5 ± 3.4	0	0	58.5 ± 2.8	0	0	82.4 ± 5.2

Hemolysis was estimated, on rabbit and human RBC, by $C_{50\%}$ and V_{lim} (upper limit of V_{max}), obtained as shown in Fig. 1. Leucotoxic activity was tested on monocytes from human blood and on two stabilised cell lines: TPH1 and RAJI. Relative efficiency was evaluated by the maximal amount of cell death in percent, and by the concentration necessary to reach half that value ($C_{50\%}$), both obtained as shown in Fig. 4. Data are average ± S.D. of at least two different experiments; 0 means there was no activity.

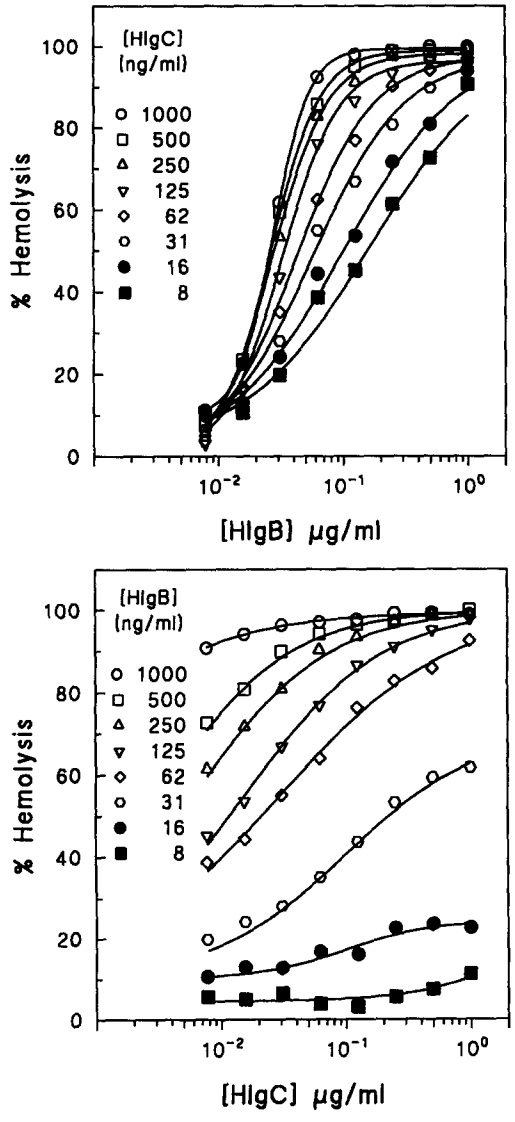

Fig. 2. Single component dose dependence of the hemolytic activity of γ-hemolysins. Percent of hemolysis was determined as in Fig. 1 except that one of the two components was held at the indicated, constant, concentration, while the other was varied. Results are exemplified by the couple HlgC+HlgB. Curves were best fit of the Hill equation. The Hill coefficients obtained were reported in Fig. 3. Experiments were performed on rabbit RBC. Reported is one single experiment of three that were performed with similar results.

Finally, since these are bi-component toxins, we studied the dependence of RRBC lysis on the concentration of each component separately. The sigmoidal titration curves (Fig. 2) suggested a co-operative behaviour, which could be compatible with an oligomerisation mechanism. The curves were fitted to the Hill equation, and the resulting Hill coefficients are reported in Fig. 3, together with that of α-toxin, as a function of the concentration of the single components.

3.2. Leucotoxic activity

The leucotoxic activity of all the possible couples was assayed. This was done on freshly isolated human monocytes and on two cultured human cell lines: THP-1 (monocytes from a newborn), and RAJI (Burkitt lymphoma cells). Results with primary monocytes are reported in Fig. 4. An assay of cell viability in the presence of different amounts of HlgA+HlgB is shown in panel A, whereas the activities of all the different toxins, as indicated by the percentage of cell death after 10 h, are compared in

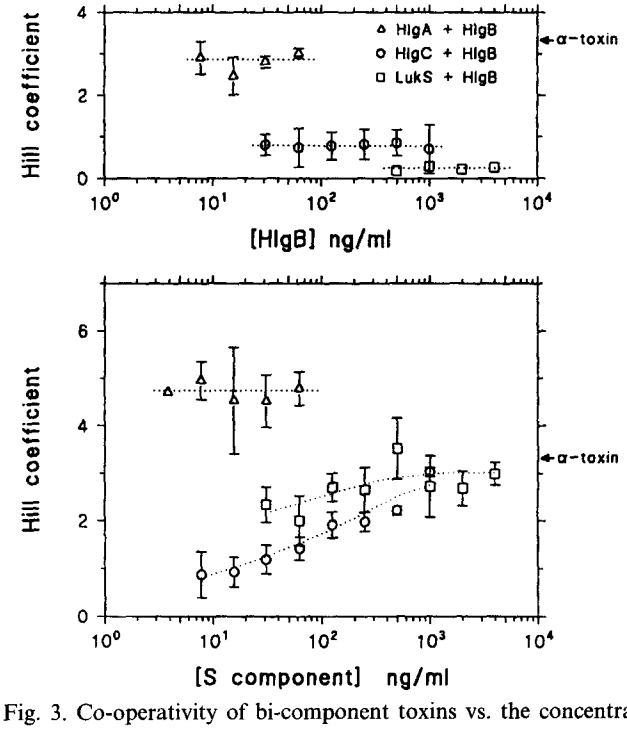

Fig. 3. Co-operativity of bi-component toxins vs. the concentration of one of the two single components. Different symbols have been used for different couples, as indicated. Hill coefficients were obtained from experiments like those in Fig. 2. Couples tested included the 3 different S-components coupled to HlgB. In the upper panel is the co-operativity in the S-component, expressed by the Hill coefficient obtained by changing the concentration of the S-component alone for every reported concentration of HlgB. In the lower panel is the co-operativity in the F-component, calculated in the same way. Points are mean ± S.D. of 2–3 experiments. Dotted lines have no theoretical significance. The Hill coefficient obtained with α-toxin is also indicated.

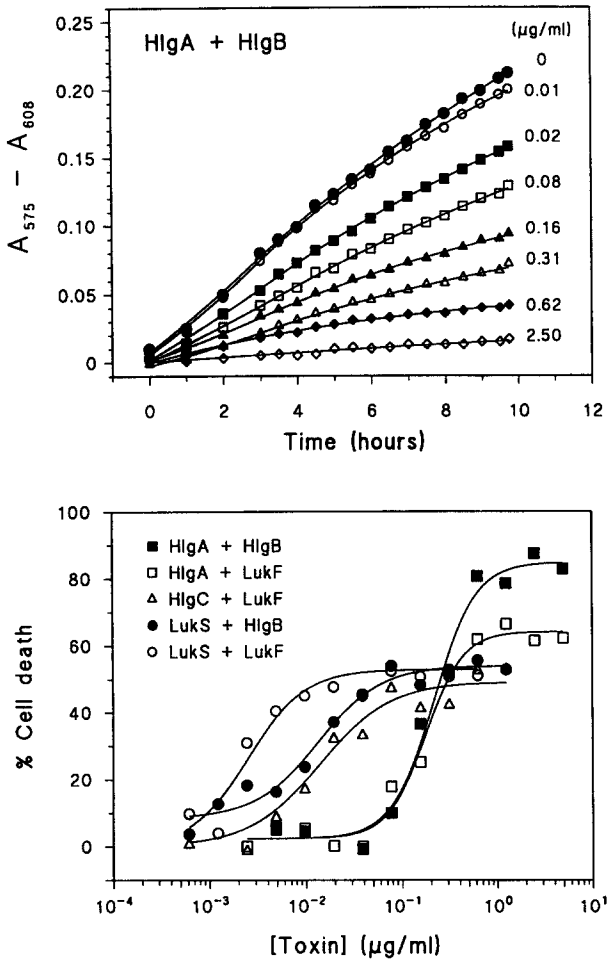

Fig. 4. Titration of the leucotoxic effect of bi-component toxins on human monocytes. A: Metabolic activity of freshly prepared human monocytes exposed to different doses of HlgA+HlgB, was determined by the differential absorption $A_{575}-A_{608}$ of alamar Blue (see Section 2). The control curve (upper one) was used as an indicator of the activity of 100% living cells. B: Extent of cell death after 10 h, obtained by comparison with the control. Different symbols have been used for different couples, as indicated. Curves were best fit of the Hill equation providing the following coefficients: HlgA+HlgB, 2.0; HlgC+HlgB, 2.9 (omitted for clarity); LukS-PV+HlgB, 1.3; HlgA+LukF-PV, 2.2; HlgC+LukF-PV, 1.2; LukS-PV+LukF-PV, 1.5. The S and F component were always applied at the same, indicated, concentration. The Hill coefficient obtained with α-toxin in a similar experiment was 1.5.
←

panel B. The couple acting at the lowest concentration was clearly LukS-PV+LukF-PV, however, HlgA+HlgB was able to kill the largest fraction of cells. The leucotoxic activity on different cell lines of the six couples plus α-toxin, as expressed by the fraction of cells that could be killed and the concentration needed for half maximal activity ($C_{50\%}$) are reported in Table 1. All these toxins presented leucotoxic activity on primary human monocytes, but surprisingly THP-1 cells, which are also a human monocytic line, were only sensitive to HlgA+HlgB, HlgA+LukF-PV and α-toxin. The same was true for RAJI cells, which is, however, a lymphocytic line.

3.3. Permeabilisation of lipid vesicles

The ability of the six bi-component toxins to permeabilise lipid vesicles comprised of PC/Cho in different proportions was next analysed. Up to the

Table 2
Composition dependence of the permeabilising activity of γ-hemolysins and α-toxin on SUV

			HlgA+HlgB	HlgC+HlgB	α-Toxin
PC/Cho	1:0	% release	1.3±0.8	3.0±1.2	0.0
		V_0 (min^{-1})	0.18±0.01	1.02±0.01	0.0
	4:1	% release	2.8±0.5	4.2±0.7	1.4±0.9
		V_0 (min^{-1})	0.42±0.02	3.42±0.06	0.30±0.05
	2:1	% release	5.1±0.5	5.2±1.2	7.9±0.9
		V_0 (min^{-1})	0.90±0.01	3.40±0.02	0.60±0.03
	1:1	% release	53.3±5.7	20.1±1.2	80.8±2.8
		V_0 (min^{-1})	37.3±1.2	11.7±0.6	37.6±2.2

SUV comprised of PC/Cho at the reported molar ratios were exposed to γ-hemolysins and α-toxin. The final concentration of any component was 3 μg/ml, that of lipid was 10 μg/ml. Permeabilisation is reported by the percentage of release, with respect to that obtained with 1 mM Triton X-100, and by V_0, the initial slope of the fluorescence change (normalised by dividing by the fluorescence after the detergent). Data are the average±S.D. of at least two different experiments.

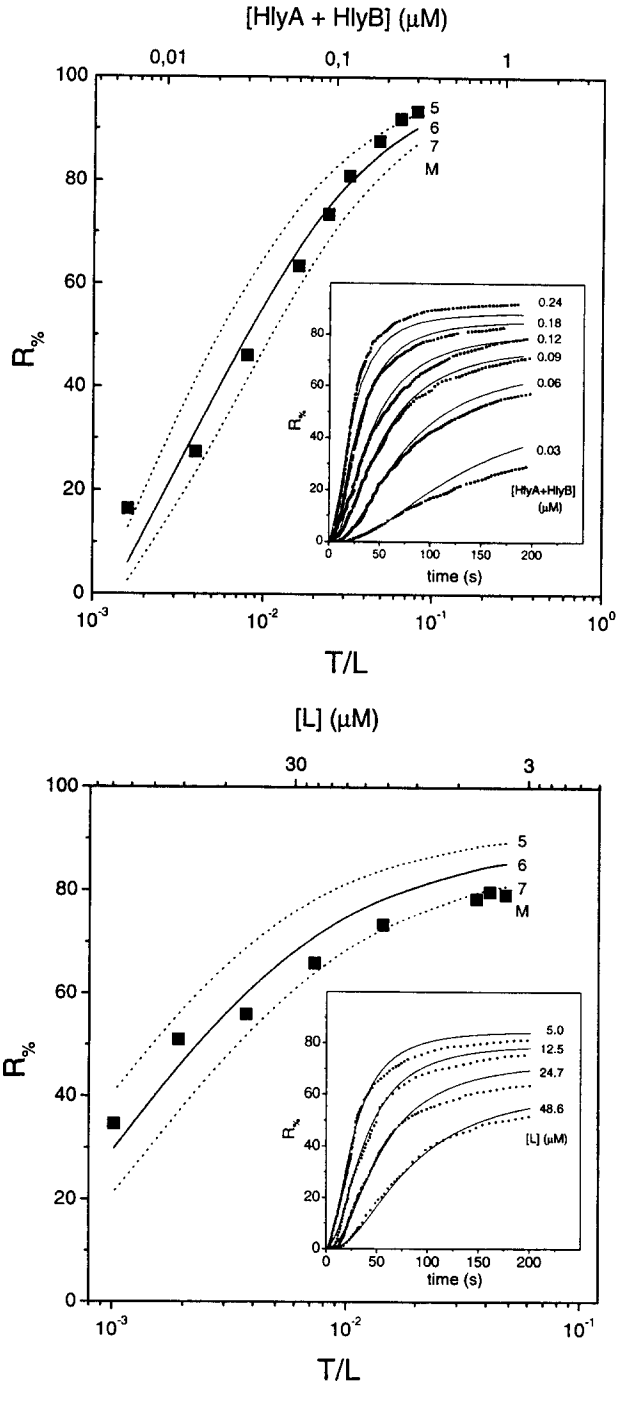

Fig. 5. Permeabilising activity of HlgA+HlgB, on SUV comprised of PC/Cho (1:1) in buffer A. Calcein release was determined, at the steady state, as a function of the toxin/lipid ratio (*T/L*) and expressed as % of the maximal value obtained with Triton X-100. In the upper panel are experiments obtained at constant lipid concentration (3.75 μM) and variable toxin concentration (the components were equimolar and the value reported is the total). In the lower panel, toxin concentration was constant (0.18 μM) and lipid was variable. *T/L* ratio and true concentrations are reported in the lower and upper scales of each panel. The solid line is a best fit of the model discussed in the text and the two dotted lines define the confidence limit for the parameter *M* (i.e. an integer representing the size of the oligomeric pore). *M* is 6 for the best fit and 7 and 5 for the upper and lower limit, respectively (as shown). In a similar way we obtained the best fit values and the confidence limits for the other two parameters of the model, i.e. the equilibrium constants for the partitioning from buffer to lipid, $K_1 = (9 \pm 4) \times 10^4$ M^{-1}, and for the aggregation within the lipid phase, $K_2 = 0.25 \pm 0.1$. It should be emphasised that these are best fit values common to the two experimental protocols. Furthermore, the confidence limits (here and below) included around 90% of the points, thus corresponding to about twice the S.D. In the two insets are the time courses of the fluorescence increase due to calcein leakage, at the indicated toxin or lipid concentrations. The solid lines are the predictions of the model using the best fit values for the three parameters *M*, K_1 and K_2 obtained from the steady-state values, and adjusting only the fourth free parameter, i.e. the forward rate for aggregation, *c*. We obtained $c = (7 \pm 2) \times 10^{-4}$ s^{-1}, and from this we calculated *d*, the backward rate for removing a monomer from the aggregate, as $d = (2.8 \pm 1) \times 10^{-3}$ s^{-1}. Once again, it should be noted that this are best fit values common between the two experiments. Other conditions are as above. With similar experiments we determined also all the constants relative to the interaction of HlgC+HlgB with the same kind of vesicles. We obtained: $M = 6 \pm 1$, $K_1 = (9 \pm 4) \times 10^4$ M^{-1}, $K_2 = 0.04 \pm 0.01$, $c = (3 \pm 2) \times 10^{-4}$ s^{-1} and $d = (7.5 \pm 5) \times 10^{-3}$ s^{-1}, which were valid both for constant lipid concentration (3.75 μM) and for constant toxin concentration (0.3 μM).

maximum concentration tested (10 μg/ml per component) only HlgA+HlgB and HlgC+HlgB were able to induce the release of calcein from the liposomes. As with α-toxin [35], permeabilisation increased with the amount of cholesterol present in the SUV (Table 2), however, the sensitivity to the presence of cholesterol was lower in the case of γ-lysins. With both active couples, and SUV containing equimolar amounts of PC and cholesterol, we determined the dependence of calcein release on the concentration of both reactants separately (Fig. 5). The experimental data were analysed in terms of a model that we have recently used [20]. It describes permeabilisation as the result of the formation of an oligomeric toxin lesion on the vesicles. The steady state effects are accounted by three parameters only: *M*, the minimal number of monomers necessary to form a lesion; K_1, the partition coefficient of the toxin between water and lipid

phase and K_2, the equilibrium constant for the aggregation of toxin monomers within the membrane.

Numerical solutions were obtained by varying independently these three parameters over a wide range of values and choosing those providing the best χ^2 values for further refinement. After a few iterations, we found the triplet giving the best fit for each couple. The level of confidence on the three parameters was estimated by comparing the predictions of the model when the parameters were changed one at a time around the best value as shown in Fig. 5 for the case of the size M. We observed that the formation of a lesion of size $M=6\pm1$ provided an adequate fit with both couples. Also the partitioning constant K_1 was the same: $(90\pm40)\times10^3$ M^{-1}. A significant difference was observed instead in the case of the aggregation constant K_2, which was 0.25 ± 0.10 with HlgA+HlgB and 0.04 ± 0.01 with HlgC+HlgB. This resulted in a lower tendency of HlgC+HlgB to aggregate on the surface of the SUV, with the overall effect that HlgA+HlgB permeabilised SUVs about 10 times better than HlgC+HlgB. Analysis of the kinetics (insets in Fig. 5) allowed estimation of c, the forward rate constant for aggregation. We obtained $c=(7\pm2)\times10^{-4}$ s^{-1} for HlgA+HlgB and $(3\pm2)\times10^{-4}$ s^{-1} for HlgC+HlgB.

3.4. Characterisation of the oligomers by SDS-PAGE

The dose-dependence of the hemolytic, leucotoxic and permeabilising activities of bi-component toxins (Figs. 1–5) suggests the formation of oligomers on the lipid membrane. This is a common mechanism for bacterial toxins, including α-toxin, however, in the case of bi-component toxins it should be clarified whether both of the toxin components are present in the oligomer, and, in that case, with what stoichiometry. To answer this, we further studied the nature of the oligomers formed by HlgA+HlgB and HlgC+HlgB on lipid vesicles. The couple LukS-PV+LukF-PV, which has no permeabilising activity, was also included in order to identify at which step it was deficient. After incubation with SUV, unbound toxins were removed by ultrafiltration. The washes were checked for the presence of free toxins, by measuring their hemolytic activity and by SDS-PAGE. With all couples the content of free toxin in the filtrates was in monomeric form and had a

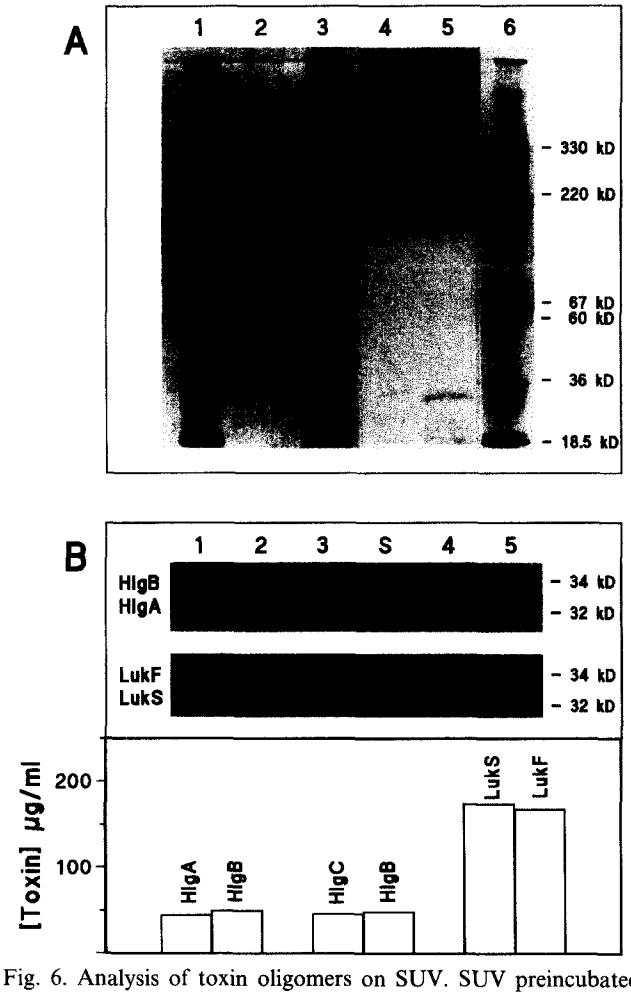

Fig. 6. Analysis of toxin oligomers on SUV. SUV preincubated with three bi-component toxins and α-toxin were washed 8 times on polysulfone filters to get free of unbound toxin and then subjected to SDS-PAGE before (panel A) or after boiling (panel B). A: Lanes 1 and 6 were M.W. standards of the indicated weight; lanes 2–5 contained α-toxin, LukS-PV+LukF-PV, HlgC+HlgB and HlgA+HlgB, respectively. Very small concentrations of monomers were detected (higher in the case of α-toxin). A high M.W. band of around 200 kDa appeared with all samples. In the case of bi-component toxins additional bands of higher mass were also present. The M.W. observed were: 190, 320, 450 and 600 kDa. B: When the lipid induced oligomers were boiled (lanes S), all of the protein migrated in only two bands with apparent M.W. 31 and 35 kDa which correspond to the mass of the single monomeric components (theoretically 32 and 34 kDa for the S- and F-component, respectively). The concentration of the two components was evaluated from the optical density of their band, by comparison with known amounts of the same component applied in lanes 1–5 (these contained 40, 80, 120, 160 and 240 µg/ml of the F-component and 240, 160, 120, 80 and 40 µg/ml of the S-component, respectively). The evaluated concentrations are reported in the lower part of the panel. Gels were stained with silver in panel A and with Coomassie blue in panel B.

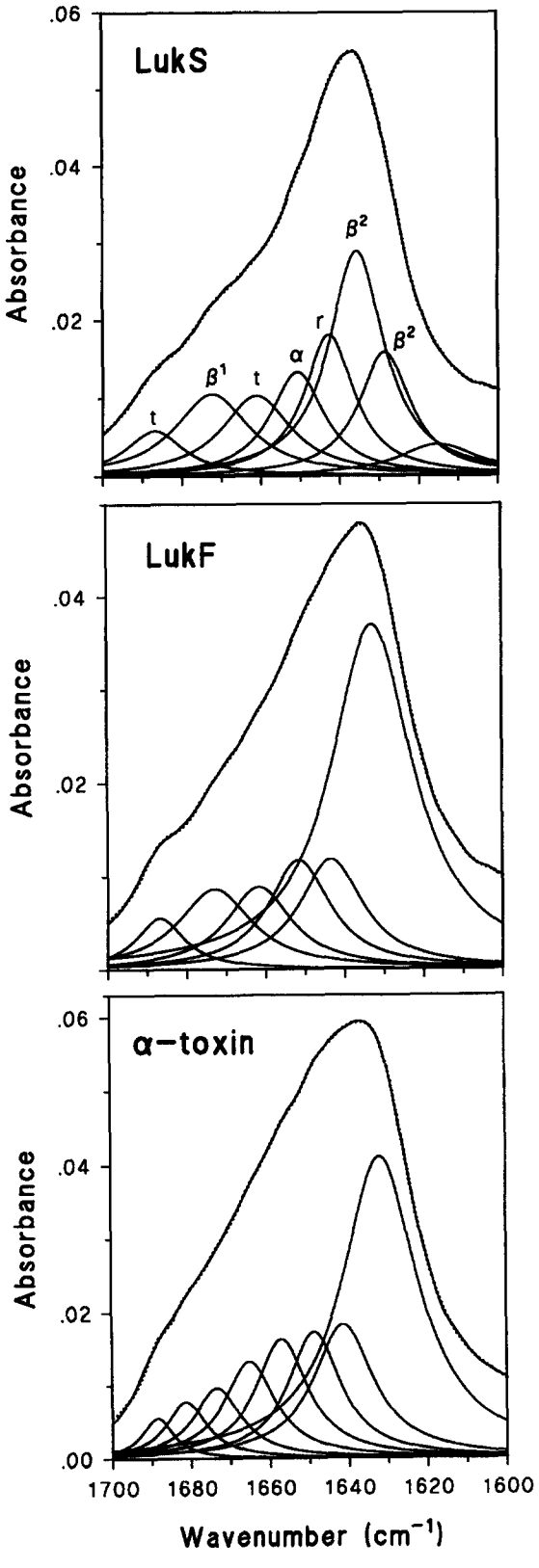

Fig. 7. Infrared-ATR spectra in the amide I′ region of deuterated films of all *S. aureus* leucotoxins investigated as single components. One class S component (LukS-PV) and one class F component (LukF-PV) are shown as examples, together with α-toxin. The spectrum (solid line), seven to eight Lorentzian component bands obtained by curve-fitting as explained in the Section 2 (thin solid lines), and their sum (dotted line) are shown in each case. Best fitted Lorentzian components were assigned to a particular secondary structure in the usual way [24,28] and the assignments are indicated next to each band for the case of LukS-PV. We used the following criteria: bands in the regions 1696–1680 cm^{-1} and 1670–1660 cm^{-1}, β–turn (t); band at 1675±4 cm^{-1}, antiparallel β-sheet (β^1); band at 1654±4 cm^{-1}, α-helix (α); band at 1645±4 cm^{-1}, random coil (r); bands in the region 1640–1620 cm^{-1}, parallel plus antiparallel β-sheet (β^2). The minor bands around 1610 cm^{-1} were attributed to side chains [29]. The evaluated secondary structures of all components are compared in Table 3.
←

peak between wash 2 and 4, thereafter declining to virtually nil at wash 8 (not shown). Eight washes were therefore used throughout. The retentates, containing SUV with bound toxins, were collected and subjected to SDS-PAGE, either with or without boiling. Unboiled samples appeared as high molecular weight proteins with no significant bands corresponding to the single components (Fig. 6A). A similar pattern was obtained with all three couples, although with HlgA+HlgB and HlgC+HlgB the bands were less intense. Despite an evident smearing, due in part to the interaction with the lipids, a few

Table 3
FTIR determination of the secondary structure of *S. aureus* leucotoxins, as single components, and α-toxin

Protein	β^1	β^2	t	α	r	β^a_{tot}
HlgA	10	52	14	9	15	76
HlgC	10	49	13	11	17	72
LukS-PV	10	50	10	9	21	70
HlgB	9	46	13	9	23	68
LukF-PV	8	49	13	14	16	70
α-Toxin	6	39	16	12	27	61
α-Toxin[b]	$\beta^1+\beta^2=56$		9	6	29	65

The secondary structure elements were calculated as shown in Fig. 7. Errors of such determinations are typically ±5%. The standard deviations derived from several independent fits were always smaller than this.
[a] β_{tot} = β-structure total = $\beta^1+\beta^2$+t.
[b] Determined by X-ray crystallography of the DOC-induced oligomer [37].

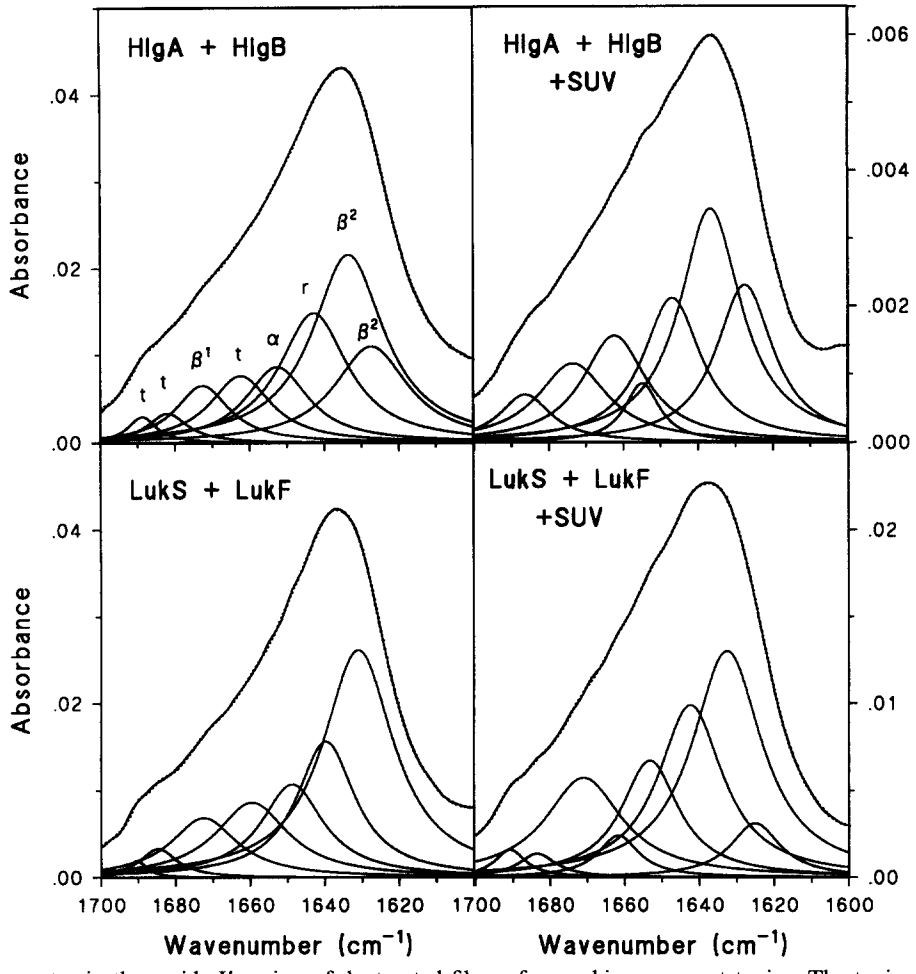

Fig. 8. Infrared-ATR spectra in the amide I′ region of deuterated films of some bi-component toxins. The toxin couples were taken either from mixtures in solution (left panels) or as SUV-bound oligomers (right panels) prepared as shown in Fig. 6. The spectrum, the fitted Lorentzian components with their assignment and their sum are shown as in Fig. 7. HlgA+HlgB and LukS-PV+LukF-PV are in the upper and lower panels, respectively. HlgC+HlgB was also analysed in the same way (not shown). All the evaluated secondary structures are reported in Table 4.

major bands could be identified, especially with LukS-PV+LukF-PV. They corresponded to molecular species around 6, 10, 14 and 18 times larger than the average molecular weight of the single components (33 kDa). The most intense band was always that near 200 kDa, similar to the α-toxin oligomer. When the samples were boiled, no oligomeric form was left, and only the two bands corresponding to the single monomeric components appeared (Fig. 6B), suggesting that this treatment splits the oligomers into the constituent monomers, as with α-toxin. These samples could therefore be used to evaluate the stoichiometry of such oligomers. The amount of each component was separately determined by comparison with a calibration obtained including in the same gel known quantities of the monomer. In this way the ratio *S/F* component was evaluated to be 0.96 ± 0.06, 0.89 ± 0.06 and 1.11 ± 0.08, for HlgA+HlgB, HlgC+HlgB and LukS-PV+LukF-PV, respectively. We could also calculate the true amount of toxin recovered, and, by comparison to the initial amount applied, the fraction of toxin that was bound to the membrane. It was found that $\approx 20\%$ of HlgA+HlgB and HlgC+HlgB, and $\approx 60\%$ of LukS-PV+LukF-PV, were retained. If the incubations were performed in the absence of SUV, all of the protein came out in monomeric form in the filtrate at the first washes and nothing was retained (not shown).

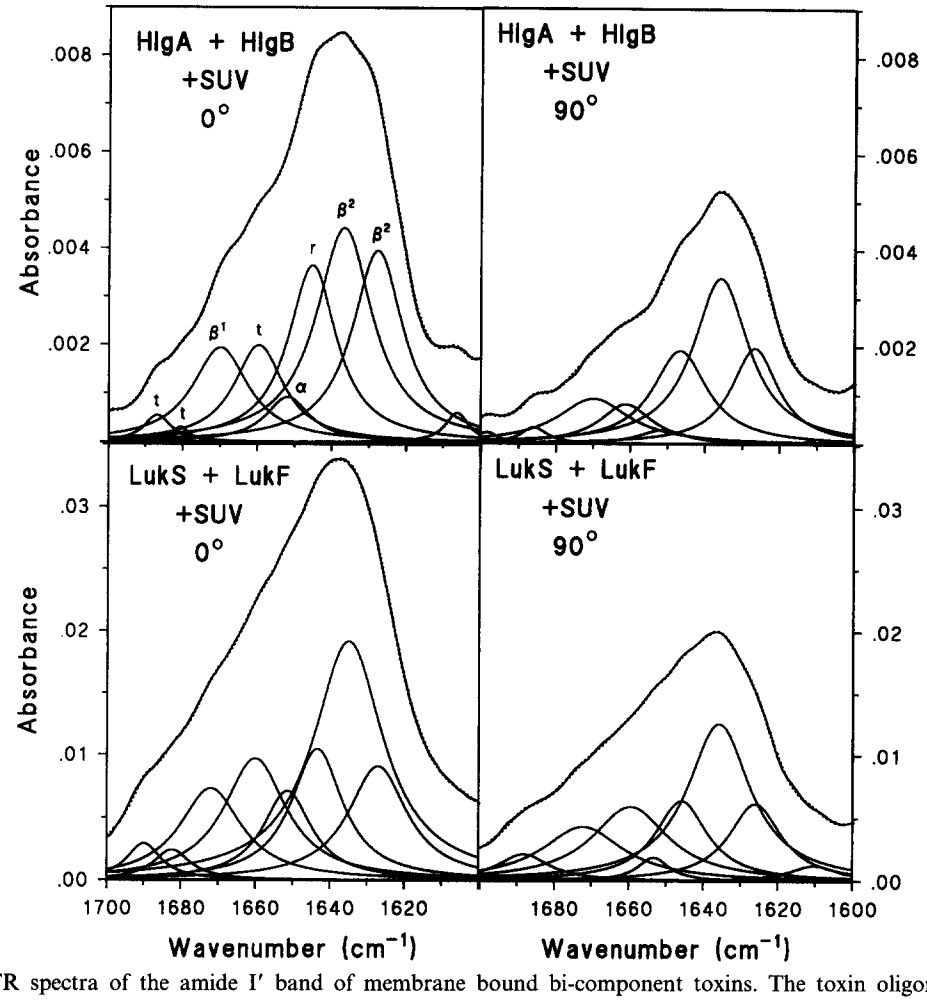

Fig. 9. Polarised ATR spectra of the amide I′ band of membrane bound bi-component toxins. The toxin oligomers analysed in the right panels of Fig. 8 were also investigated using linearly polarised light. Polarisation was either parallel (left panels) or perpendicular (right panels) to the plane of the internal reflections. The spectrum, the fitted Lorentzian components with their assignment and their sum are shown as in Figs. 7 and 8. HlgA+HlgB and LukS-PV+LukF-PV are in the upper and lower panels, respectively. HlgC+HlgB was also analysed in the same way, but not shown. The dichroic ratio $R_\beta = A_{\beta\parallel}/A_{\beta\perp}$ (where β means $\beta^1+\beta^2$) was 1.58±0.05, 1.56±0.04 and 1.60±0.05 for HlgA+HlgB, HlgC+HlgB and LukS-PV+LukF-PV, respectively.

3.5. *Secondary structure of bi-component toxins by FTIR spectroscopy*

The secondary structure of all single components was estimated by ATR-FTIR spectroscopy, and compared to that of α-toxin (see examples in Fig. 7). Spectra were fitted to the sum of single Lorentzian bands and these were attributed, according to the standard interpretation [28], to four secondary structures, i.e. β-turn, α-helix, random coil and β-sheet. The last is split in two bands, called β^1 and β^2, that contain the contribution from antiparallel and from parallel+antiparallel β-strands, respectively. Average compositions are reported in Table 3. It appears that all proteins in the family were mainly composed of β-structure. In particular, the spectra of the class-S components were very similar to each other, and had the highest content in β-structure of the group. Those of the class-F components were also very homogeneous, but slightly different from the previous. Finally, that of α-toxin was the most dissimilar, yet still closely related to that of the class-F components. This reflected well the phylogenetic subdivision inside this group of proteins [3,36]. The determined secondary structure of α-toxin was compared to that derived from the crystallographic analysis of the oligomer it forms in DOC [37] and found to be consistent.

To get some insight into the conformational changes that might accompany the formation of the pore we evaluated the secondary structure of the oligomers formed in SUV by the three couples previously analysed by SDS-PAGE, and compared it either to that of the same couples in solution or to a simple average of the two single component structure. Only minor changes were observed in the differential spectra, i.e. an excess of absorbance in the 1680–1660 cm^{-1} region in the case of HlgA+HlgB and HlgC+HlgB, but much less with LukS-PV+LukF-PV. This was consistent with a slight increase in β-structure and decrease of α-helix evidenced for the γ-lysins by curve fitting (Fig. 8 and Table 4). Spectra collected using light linearly polarised at 90° (Fig. 9) allowed to evaluate the *L/T* ratio in each of the lipid-bound toxin samples (see Section 2). *L/T* values of 620 ± 40, 580 ± 40 and 310 ± 20 were obtained for HlgA+HlgB, HlgC+HlgB and LukS-PV+LukF-PV, respectively. They compared nicely to the upper bounds of 1000, 1000 and 330 that could be evaluated for the same samples using the protein concentration measured by SDS-PAGE (Fig. 6B) and assuming that all of the lipid was recovered by the ultrafiltration process. Finally, from polarisation experiments, we could also evaluate the average orientation of the oligomers in the bilayer (Fig. 9). Using the same technique that was applied to porins [34], we estimated that the average angle formed by the β-strands ($\beta^1+\beta^2$ bands) with the normal to the plane of the membrane, was 37° ± 1°, 36° ± 1° and 38° ± 1° for HlgA+HlgB, HlgC+HlgB and LukS-PV+LukF-PV, respectively.

Table 4
Secondary structure of *S. aureus* bi-component toxins in solution and in membrane-bound form

Protein	β^1	β^2	t	α	r	β_{tot}
⟨HlgA+HlgB⟩[a]	9	50	14	9	19	72
HlgA+HlgB[b]	7	50	13	12	18	70
$(HlgA+HlgB)^c_{ves}$	12	49	17	4	18	78
⟨HlgC+HlgB⟩	10	47	13	10	20	70
HlgC+HlgB	11	46	13	8	22	70
$(HlgC+HlgB)_{ves}$	14	39	21	4	22	74
⟨LukS+LukF⟩	9	50	12	11	18	71
LukS+LukF	9	40	16	15	20	65
$(LukS+LukF)_{ves}$	16	39	8	14	23	63

The secondary structure elements were calculated as shown in Fig. 8 and Table 3.
[a]⟨S+F⟩ is the averaged structure of the indicated S and F component, as taken from Table 3.
[b]S+F is the structure of an equimolar mixture of the two components S and F in solution, obtained as shown in Fig. 8.
[c]$(S+F)_{ves}$ is the structure of the oligomer formed by the two components S and F on lipid vesicles.

4. Discussion

All possible bi-component combinations between *S. aureus* PVLs and γ-hemolysins were analysed for activity on RBC, leukocytes, and model membranes. Couples involving HlgB presented hemolytic activity on RRBC (Fig. 1 and Table 1), including that with LukS-PV, a combination previously reported as non-hemolytic [15]. Conversely, LukF-PV was slightly hemolytic only in combination with HlgA. The sigmoid dose-dependence of the hemolytic activity of these bi-component toxins suggests that their action relies on the formation of an oligomer, as in the case of α-toxin. With all the hemolytic couples, and both on RRBC or HRBC, the S component was the first to bind to the membrane, whereas the F component was never able to bind to the cell if the S component was not present (Table 2). This is in agreement with most previous results [6,7], but contrasts to those reported by a group for the case of HlgA+HlgB on HRBC [8,9]. We do not have at present any reasonable explanation for this disagreement, however, we notice that our results provide a more consistent behaviour for all the toxins within this family.

The observed sequentiality suggests that the S component may bind to a receptor. To distinguish between the respective role of the S and F components, we studied their individual contribution to the co-operativity in hemolysis (Figs. 2 and 3). The co-operativity in the binding of the S component is lower than that of the F component. In particular, LukS-PV presents negative co-operativity (Hill coefficient, *H*, around 0.2), HlgC no co-operativity (*H* around 1), whereas HlgA is the only one with a positive co-operativity (*H* around 3). Apart from HlgA, these values are consistent with a non-co-operative (or even competitive) binding to a receptor, indicated also by the fact that the co-operativity of the S component does not depend on the concentra-

tion of the F component. The peculiarity of HlgA is probably due to the fact that, as we had previously demonstrated [16], it may also bind non-specifically to the cell membrane. The co-operativity with the F component (HlgB) is higher, and, except with HlgA, dependent on the concentration of the S component. The upper value of H is between 3 and 4 suggesting the formation of an oligomer comprising 3 or 4 HlgB monomers and requiring a sufficient amount of the S component for full development.

The pore-forming action of α-toxin involves at least three consecutive steps: binding of monomers to the erythrocyte membrane; assembly of a non-lytic oligomer; reorganisation into a functional ion channel [38–41]. It has been shown that the first step is temperature-independent, whereas the later events require temperature. We observed the same situation also for leucocidins and γ-hemolysins. Both S and F components can bind to RBC membrane at 0°C, but are unable to generate a lytic lesion, unless the medium containing cells and bound toxins is warmed up. HlgA+LukF-PV, alone, presented an activity higher at 20°C than at 37°C, as observed earlier for α-toxin [42]. These facts suggest that the mechanism of action of leucocidins and γ-hemolysins also involves several independent steps, at least the binding of toxin monomers and a further structural reorganisation leading to the final pore.

All the couples were leucotoxic on primary human monocytes (Fig. 4 and Table 1). Couples based on either LukS-PV or HlgC were active at low doses (LukS-PV+LukF-PV was the most active based on $C_{50\%}$), but were able to kill only around 50% of the cells, whereas couples containing HlgA required higher doses, but could kill almost all the cells. This suggests that LukS-PV and HlgC require a receptor that is not present on all monocytes in the preparation, or on some other white cells that might remain in the culture. Interestingly, only couples based on HlgA were toxic for THP1 and RAJI cells, although TPH1 cells are also monocytes. Hill coefficients for the leucotoxic activity were in the range 1.2–2.9, confirming a positive co-operativity also for this effect.

The activity in the absence of any specific receptor was investigated using SUV as a model membrane (Fig. 5). HlgA+HlgB and HlgC+HlgB (the γ-hemolysins) indeed presented permeabilising activity, similar to that of α-toxin, HlgA+HlgB being the most active. This confirmed that at least HlgA and HlgC could bind to the lipid membrane directly and cooperate with HlgB (but not with LukF-PV) to form a pore. All couples with LukS-PV were inactive on SUV, at least at the concentrations tested. Statistic analysis of the permeabilising activity of the γ-hemolysins (Fig. 5) suggested that the lesions were formed by hexamers. Such oligomers could be shown directly by SDS-PAGE, but unexpectedly, besides with HlgA+HlgB and HlgC+HlgB, they were also observed with LukS-PV+LukF-PV (Fig. 6A) in an even higher proportion. This indicates that LukS-PV and LukF-PV were also able to bind to the membrane and to assemble the oligomer, albeit not to permeabilise the vesicles. Thus, the defective step could be the lack of a conformational change of the preassembled oligomer into a calcein-permeant channel. Unlike the oligomer formed by α-toxin in deoxycholate, which is a heptamer [37], the major oligomeric species appearing on the membrane of the liposomes was a hexamer. Furthermore, within experimental error, the stoichiometry of the two different components in the oligomer was 1:1 (Fig. 6B), implying that both the S and F components were present in the same extent, which would not be possible for a heptamer. This hexameric nature is not unexpected since: (i) oligomers of γ-lysins observed by others on RBC were indeed found to be hexamers [12]; (ii) α-toxin itself apparently can form hexamers besides heptamers on phospholipid bilayers [41]. Interestingly, with γ-lysins incomplete rings, harbouring four subunits and attached to the complete hexamers, were also observed on RBC [12]. They could correspond to the forms comprising 10 and 14 monomers that we have seen in SDS-PAGE.

Although sequence homology suggests that γ-lysins, PVL and α-toxin may have a similar secondary structure [36], the overall identity is always below 30% and henceforth a direct experimental demonstration of such similarity is required. We found by FTIR spectroscopy that indeed bi-component toxins have a secondary structure consisting prevalently of β-sheet and turn, similar to that of α-toxin. No major changes were observed upon formation of the membrane-bound oligomers with respect to an equimolar mixture of the two components in water, or a simple mean of the two individual structures. Polar-

isation experiments indicated that the average orientation of the β-strands in the oligomers is similar to that in the porins, which would also be compatible with the formation of an α-toxin like channel [37]. The oligomer formed by the PVL, despite having an overall structure and orientation similar to that of γ-hemolysins, did not show a minor increase in β structure and decrease in α structure that was apparent with those. Although one should be cautious about these differences because they are near to the resolution limit of the technique, they would be compatible with a multistep mechanism of action similar to that of α-toxin: monomers bind to the membrane, they form an inactive oligomer which, in the case of γ-hemolysins but not of leucocidins, experiences a further (small) conformational change to become a functional lesion in the form of a pore. These findings also suggest that the in vivo leucotoxic activity of LukS-PV+LukF-PV might involve a different mechanism, e.g. the interaction with endogenous cell proteins for pore formation that was shown recently, [14,43].

Acknowledgements

This work was financially supported by the Italian Consiglio Nazionale delle Ricerche (CNR), by the Istituto Trentino di Cultura (ITC), by the French Direction de la Recherche et des Etudes Doctorales and by a grant of the European Community to G.M. (European Project CRHX-CT93-055). We appreciate the skilful technical assistance of D. Keller. M.F. and F.H. were supported by a post-doctoral fellowship of the European Community (European Project CRHX-CT93-055).

References

[1] G. Menestrina, G. Schiavo, C. Montecucco, Mol. Asp. Med. 15 (1994) 79–193.
[2] P.N. Panton, M.C. Camb, F.C.O. Valentine, M.R.C.P. Lond, Lancet I (1932) 506–508.
[3] P. Couppié, G. Prévost, Ann. Dermatol. Venereol. 124 (1997) 740–748.
[4] G. Supersac, G. Prévost, Y. Piémont, Infect. Immun. 61 (1993) 580–587.
[5] J. Cooney, Z. Kienle, T.J. Foster, P.W. O'Toole, Infect. Immun. 61 (1993) 768–771.
[6] M. Noda, T. Hirayama, I. Kato, F. Matsuda, Biochim. Biophys. Acta 633 (1980) 33–44.
[7] D.A. Colin, I. Mazurier, S. Sire, V. Finck-Barbançon, Infect. Immun. 62 (1994) 3184–3188.
[8] T. Ozawa, J. Kaneko, Y. Kamio, Biosci. Biotech. Biochem. 59 (1995) 1181–1183.
[9] J. Kaneko, T. Ozawa, T. Tomita, Y. Kamio, Biosci. Biotech. Biochem. 61 (1997) 846–851.
[10] Noda, M. and Kato, I. (1991) in: Sourcebook of Bacterial Protein Toxins (Alouf, J.E. and Freer, J.H., Eds.) pp. 243–251, Academic Press, London.
[11] V. Finck-Barbancon, G. Duportail, O. Meunier, D.A. Colin, Biochim. Biophys. Acta 1182 (1993) 275–282.
[12] N. Sugawara, T. Tomita, Y. Kamio, FEBS Lett. 410 (1997) 333–337.
[13] T. Hensler, B. König, G. Prévost, Y. Piémont, M. Köller, W. König, Infect. Immun. 62 (1994) 2529–2535.
[14] O. Meunier, A. Falkenrodt, H. Monteil, D.A. Colin, Cytometry 21 (1995) 241–247.
[15] G. Prévost, B. Cribier, P. Couppié, P. Petiau, G. Supersac, V. Finck-Barbançon, H. Monteil, Y. Piémont, Infect. Immun. 63 (1995) 4121–4129.
[16] O. Meunier, M. Ferreras, G. Supersac, F. Höper, L. Baba-Moussa, H. Monteil, D.A. Colin, G. Menestrina, G. Prévost, Biochim. Biophys. Acta 1326 (1997) 275–286.
[17] S. Cauci, R. Monte, M. Ropele, C. Missero, T. Not, F. Quadrifoglio, G. Menestrina, Mol. Microbiol. 9 (1993) 1143–1155.
[18] B. Pagé, M. Pagé, C. Nöel, Int. J. Oncol. 3 (1993) 473–476.
[19] C. Kayalar, N. Duzgunes, Biochim. Biophys. Acta 869 (1986) 51–56.
[20] S. Anzlovar, M. Dalla Serra, M. Dermastia, G. Menestrina, Mol. Plant-Microbe Interact. 11 (1998) 610–617.
[21] R.A. Parente, S. Nir, F.C. Szoka Jr., Biochemistry 29 (1990) 8720–8728.
[22] D. Rapaport, R. Peled, S. Nir, Y. Shai, Biophys. J. 70 (1996) 2502–2512.
[23] U.K. Laemmli, Nature 227 (1970) 680–685.
[24] E. Goormaghtigh, V. Cabiaux, J.-M. Ruysschaert, Eur. J. Biochem. 193 (1990) 409–420.
[25] U.P. Fringeli, H.H. Günthard, Mol. Biol. Biochem. Biophys. 31 (1981) 270–332.
[26] J.L. Arrondo, A. Muga, J. Castresana, F.M. Goñi, Prog. Biophys. Mol. Biol. 59 (1993) 23–56.
[27] Goormaghtigh, E., Cabiaux, V. and Ruysschaert, J.-M. (1994) in: Subcellular Biochemistry, Vol. 23: Physicochemical Methods in the Study of Biomembranes (Hilderston, H.J. and Ralston, G.B., Eds.) pp. 363–403, Plenum Press, New York, NY.
[28] D.M. Byler, H. Susi, Biopolymers 25 (1986) 469–487.
[29] S.A. Tatulian, P. Hinterdorfer, G. Baber, L.K. Tamm, EMBO J. 14 (1995) 5514–5523.
[30] Harrick, N.J. (1967) Internal Reflection Spectroscopy, Harrick Scientific Corporation, Ossining, NY.

[31] P.H. Axelsen, B.K. Kaufman, R.N. McElhaney, R.N.A.H. Lewis, Biophys. J. 69 (1995) 2770–2781.
[32] M.J. Citra, P.H. Axelsen, Biophys. J. 71 (1996) 1796–1805.
[33] L.K. Tamm, S.A. Tatulian, Biochemistry 32 (1993) 7720–7726.
[34] N.A. Rodionova, S.A. Tatulian, T. Surrey, F. Jähnig, L.K. Tamm, Biochemistry 34 (1995) 1921–1929.
[35] S. Forti, G. Menestrina, Eur. J. Biochem. 181 (1989) 767–773.
[36] E. Gouaux, M. Hobaugh, L.Z. Song, Protein Sci. 6 (1997) 2631–2635.
[37] L. Song, M.R. Hobaugh, C. Shustak, S. Cheley, H. Bayley, J.E. Gouaux, Science 274 (1996) 1859–1866.
[38] B. Walker, O. Braha, S. Cheley, H. Bayley, Chem. Biol. 2 (1995) 99–105.
[39] S. Bhakdi, H. Bayley, A. Valeva, I. Walev, B. Walker, M. Kehoe, M. Palmer, Arch. Microbiol. 165 (1996) 73–76.
[40] A. Valeva, I. Walev, M. Pinkernell, B. Walker, H. Bayley, M. Palmer, S. Bhakdi, Proc. Natl. Acad. Sci. USA 94 (1997) 11607–11611.
[41] D.M. Czajkowski, S. Sheng, Z. Shao, J. Mol. Biol. 276 (1998) 325–330.
[42] A. Hildebrand, M. Pohl, S. Bhakdi, J. Biol. Chem. 266 (1991) 17195–17200.
[43] Staali, L., Monteil, H. and Colin, D.A. (1998) J. Membrane Biol. 162.